Research and design the taper angle of a single use piston

Ngo Tien Sy*, Ho Van Khanh

Weapon Institute, Vietnam Defence Industry.
*Corresponding author: ngotiensy@gmail.com
Received 28 Nov 2022; Revised 6 Feb 2023; Accepted 10 Apr 2023; Published 28 Apr 2023.
DOI: https://doi.org/10.54939/1859-1043.j.mst.86.2023.165-172

ABSTRACT

In this paper, using numerical simulation combined with experiment, the most suitable design for piston taper angle in the single use piston of the piston - cylinder system has been proposed. The research process shows that, when the piston has a taper angle of 12^o for the design of the cylinder tail taper angle of 20^o, the resulting deformation, the equivalent stress of the cylinder tail is the smallest as well as the deceleration time of the piston is the greatest, thereby increasing the tightness and minimizing the impact of the piston-cylinder collision on the sealing process and the operational reliability of the system. The results after the study are proven experimentally, the experimental results show that the simulation results are reliable and highly applicable. The results of the article are applied to manufacturing and testing 82 mm silent mortar systems.

Keywords: Single use Piston; Piston - cylinder; Taper angle; Cylinder; Deformation.

1. INTRODUCTION

Unlike other piston and cylinder systems [1, 2], single use piston and cylinder systems are less frequently mentioned in published studies. With high pressure acting on the inner surface of the cylinder and impact velocity between piston and cylinder up to 130 m/s, single use piston and cylinder system design has to solve problems of the material used for the cylinder, impact conditions and taper angles of the piston and cylinder tail to ensure that the cylinder do not break or deform too much during operation.

Currently, many popular software can solve the impact problems with many different boundary conditions, such as: high velocity and pressure acting on the system, in which Ansys software has confirmed position in the fields of scientific research with the advantages of suitable price, ease to use and accurate results. The problem uses the explicit dynamic method to determine the influence of the taper angles 2α on the impact process between the piston and the cylinder tail. The taper angle of the cylinder tail is inherited from the previous study [3] to match the existing technological equipment and manufacturing technology.

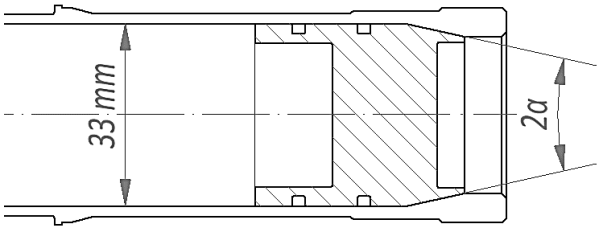

Figure 1. *Impact between piston and cylinder tail.*

In this study, the effect of the piston taper angle on the piston-cylinder impact, the equivalent stresses as well as the cylinder tail deformation are presented.

2. PISTON TAPER ANGLE DETERMINATION USING SIMULATION

In this study, data of the material properties used for the Johnson cook strength models determination were carried out by the Weapon Institute in Ha Noi. The schematic diagram of the

design process is shown in figure 2. The values of 2α taper angle are: 10°, 12°, 15°, 20° and taper angle of cylinder tail is 20°.

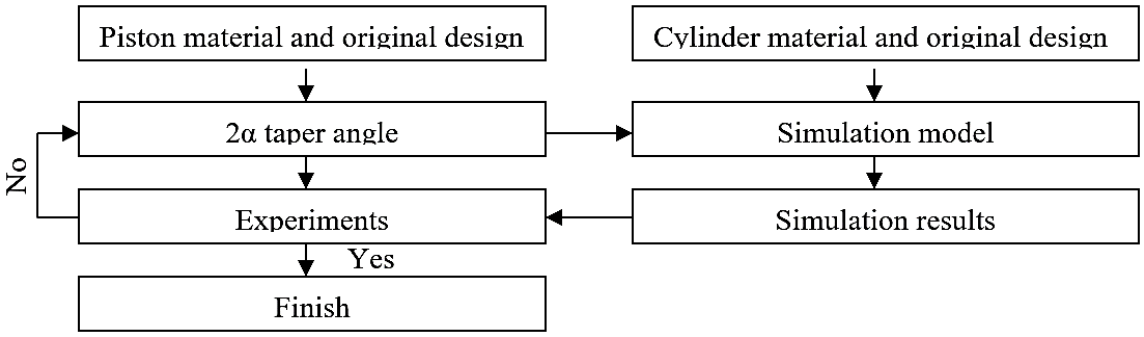

Figure 2. *Schematic diagram of the design process.*

2.1. Basic formulations for explicit dynamic FEM

FEM simulates physical phenomena by converting a continuum into a discrete domain (nodes and elements). The discrete equations of motion for the explicit dynamic FEA can be derived from the work balance contributed by the external load, inertial and viscous effects, and strain energy [4-6]. For a single element subjected to body force, surface traction, and point load, the work balance of the element is given by Eq. (1):

$$\int\{\delta u\}^T\{f\}dV + \int\{\delta u\}^T\{t\}dS + \sum_{i=1}^{n}\{\delta u\}_i^T\{p\}_i = \int(\{\delta u\}^T\rho\{\ddot{u}\} + \int\{\delta u\}^T c\{\dot{u}\} + \{\delta\varepsilon\}^T\{\sigma\})dV \quad (1)$$

where the first, second and third terms on the left hand side denote the work done by the body force $\{f\}$, surface traction$\{t\}$ and the concentrated load $\{p\}$ respectively; whereas the first, second and third terms on the right hand side denote thework done by inertial effect, viscosity, and strain energy respectively; the notation {} represents a vector; $\{\delta u\}$ is the virtual displacement; $\{\delta\varepsilon\}$ is the corresponding strain to the virtual displacement; and $\{u\}$ is the displacement which is function of space and time.

The displacement $\{u\}$ over an element can be represented by the interpolating functions and nodal degree-of-freedom (DOF) as in Eq. (2):

$$\{u\} = [N]\{x\} \quad (2)$$

where the space-dependent interpolation (or shape) function matrix $[N]$ can be determined according to the element types; and $\{x\}$ is the nodal DOF dependent on time only. With the aid of interpolation functions, strain and stress are given by Eq. (3a) and (3b) respectively.

$$\{\varepsilon\} = [B]\{x\} \quad (3a)$$

$$\{\sigma\} = [E]\{\varepsilon\} = [E][B]\{x\} \quad (3b)$$

where $[B]$ is a strain-displacement matrix (space derivative of the interpolation function matrix $[N]$); and $[E]$ is a stress–strain matrix. With Eq. (2) and (3a), (3b), Eq. (1) can be rewritten as (4) in terms of element mass, damping, and stiffness matrices as well as the external load, which are denoted by $[m]$, $[c]$, $[k]$ and $\{r_{ext}\}$ respectively in Eqs. (4a)–(4d):

$$[m]\{\ddot{x}\} + [c]\{\dot{x}\} + [k]\{x\} = \{rext\} \quad (4)$$

$$[m] = \int \rho[N]^T\,[N]dV \quad (4a)$$

$$[c] = \int c[N]^T\,[N]dV \quad (4b)$$

$$[k] = \int[B]^T[E]\,[B]dV \quad (4c)$$

$$\{rext\} = \int[N]^T[F]dV + [N]^T[t]dS + \sum_{i=1}^{n}\{\boldsymbol{p}\}_i \quad (4d)$$

2.2. Model and boundary conditions

The physical model is built, including: cylinder and piston at the immediate moment before impact. The calculating model is established based on the physical model. Because of the symmetry of the physical model, the 1/2 three-dimensional model is established, as shown in figure 3. In this article, the calculating model is regular and there is no difference in mesh density for the model, so uniform three-dimensional solid elements were used to mesh the calculating model.

Figure 4 shows the boundary conditions of the simulation problem. Boundary conditions are developed based on the basic tactical specifications of the piston and cylinder system. At the moment of impact, the piston has a velocity of 130 m/s and the pressure acting on the inner surface of the cylinder is 50 MPa. The problem uses the assumption that just before the impact between the piston and cylinder, the piston is not tilted and deformed.

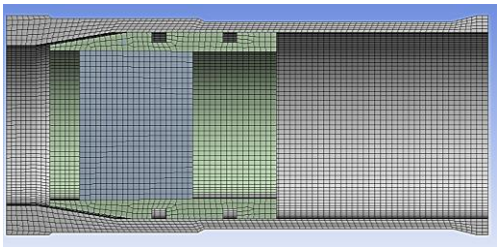

Figure 3. *The calculating model.*

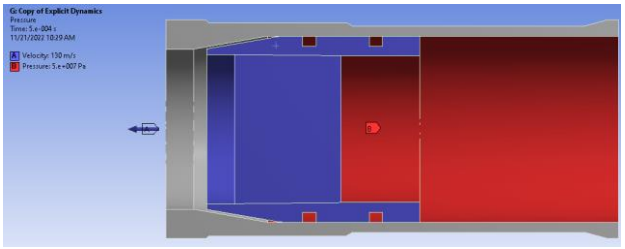

Figure 4. *The boundary conditions of the simulation problem.*

2.3. Materials used in the model

40X steel after heat treatment is used for the cylinder material and D16T aluminum is used for the piston. Table 1 shows some mechanical properties of the cylinder material tested on 03 samples.

Table 1. *Material properties of the cylinder.*

Nº	Yeild strength (MPa)	Ultimate strength (MPa)
1	1036	1180
2	1031	1178
3	1030	1176

The engineering stress-strain curve for the cylinder material gives the relationship between stress and strain, as shown in figure 5. From the stress-strain curve, the true stress-strain curve is calculated and shown in figure 5.

In this paper, Johnson and Cook material strength models are used to describe the properties of materials. From the experimental values shown in table 1 combined with calculated method , the material properties for 40X steel after heat treatment is built as follows.

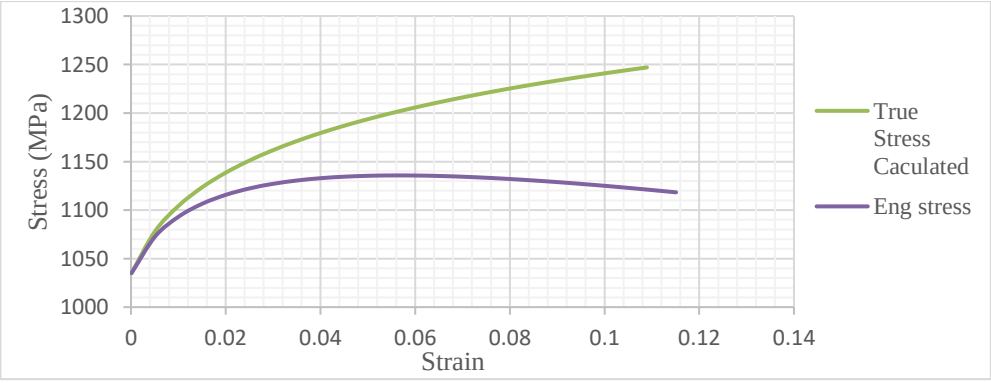

Figure 5. *Engineering stress strain curve and true stress strain curve.*

Table 2. *Material properties of cylinder.*

Nº	**Name**	**Value**	**Unit**
1	Density	7800	Kg/cm^3
2	Shear Modulus	81.8	GPa
3	Elastic modulus	2.1e11	Pa
4	Specific Heat	477	J/(kgK)
5	Yield strength	1032	MPa
6	Hardening constant	1421	MPa
7	Hardening exponent	0.08	-
8	Strain rate constant	0.012	-
9	Melting temperature	1490	ºC

D16T aluminum material is used to research, design and manufacture piston. This is the widely used material in current research and design, the material properties of the piston are presented in table 3.

Table 3. *Material properties of piston.*

Nº	**Name**	**Value**	**Unit**
1	Density	2770	Kg/cm^3
2	Shear Modulus	2.86e10	Pa
3	Specific Heat	875	J/(kgK)
4	Yield strength	395	MPa
5	Hardening constant	343	MPa
6	Hardening exponent	0.18	-
7	Melting temperature	946	ºC

3. SIMULATION RESULTS AND DISCUSSION

3.1. Simulation results

Ansys Explicit dynamic module [7] is used to solve the piston-cylinder impact problem with the assumptions presented above. The deformation values of the cylinder tail as well as the equivalent stress value of the cylinder tail are determined.

Figure 6 shows the result of the impact between the piston and the cylinder tail. The simulation results show that on the cylinder the dangerous position is the bottom of the cylinder tail (position B). When the piston decelerates to zero, it is also the time when the cylinder is the most deformed. If the deformation of the cylinder is too large, it may cause breakage and cracking of the cylinder during operation. Figure 7 shows the deformation of the cylinder after the end of the impact.

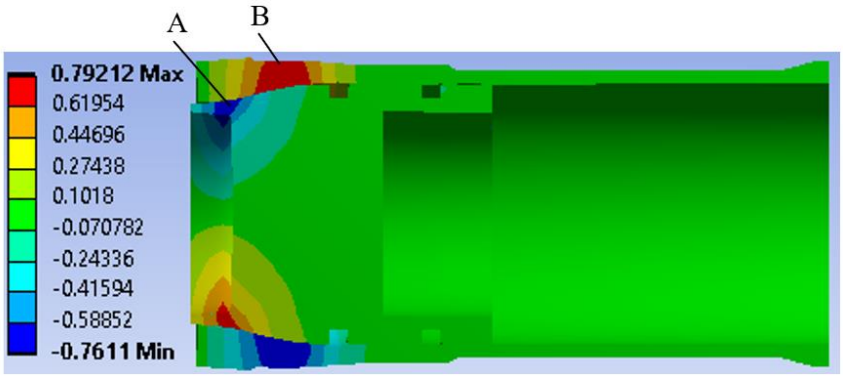

Figure 6. *The result of the impact between the piston and the cylinder tail.*

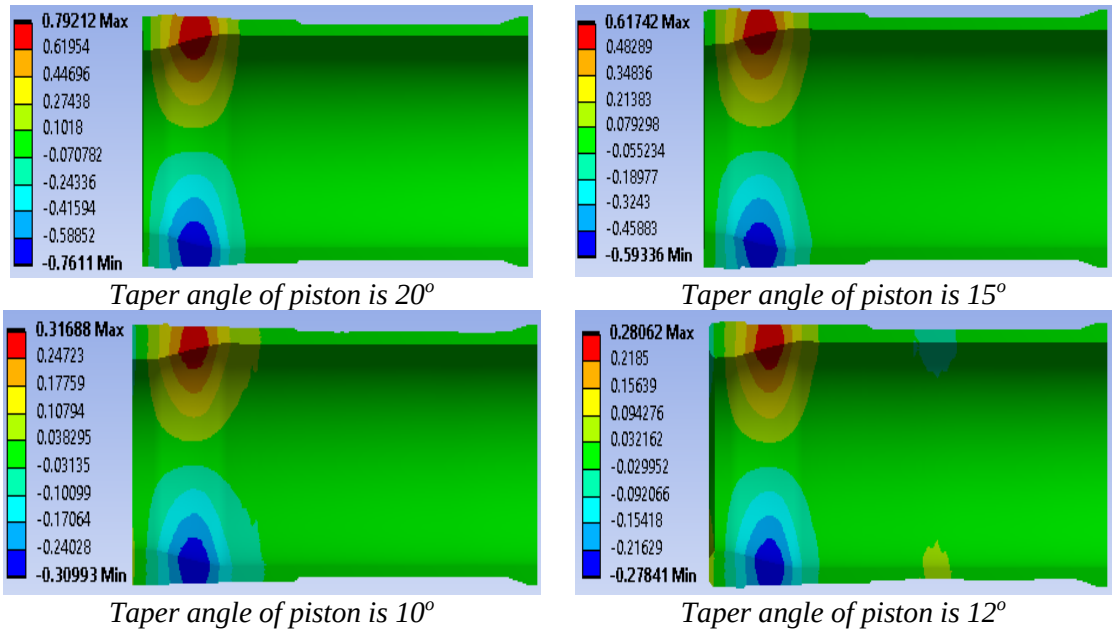

Taper angle of piston is 20º *Taper angle of piston is 15º*

Taper angle of piston is 10º *Taper angle of piston is 12º*

Figure 7. *Cylinder deformation for different piston taper angles.*

Figure 8, figure 9 show the deformation at position B of the cylinder tail when the piston is designed with different taper angles. It can be seen that with the taper angle of 12 degrees, the radial and axial deformation of the cylinder are the smallest: 0.28 and 0.105 mm. Figure 10 shows the equivalent stress of the cylinder with different piston taper angles. The maximum equivalent stress value is 1232 MPa in the case of 20 degrees piston taper angle.

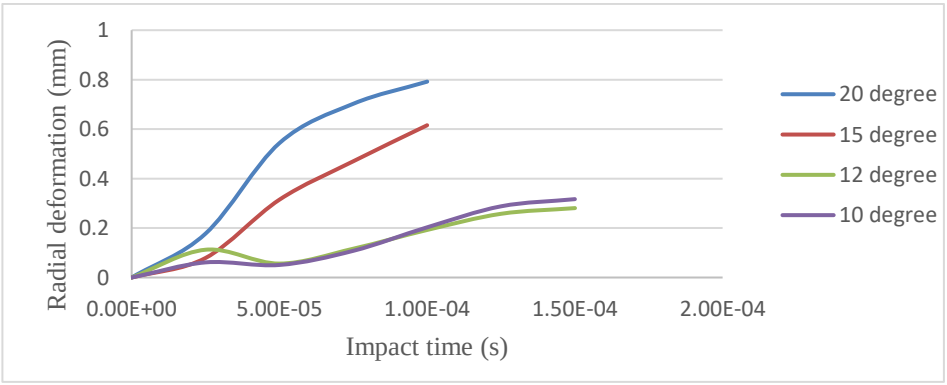

Figure 8. *The radial deformation of the cylinder vs impact time.*

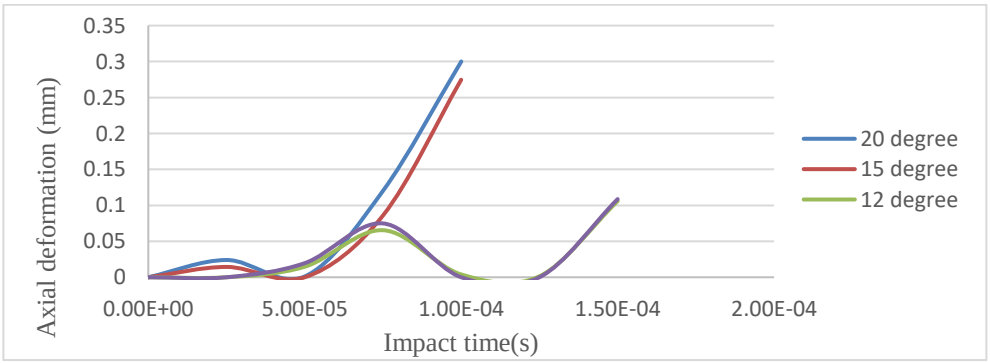

Figure 9. *The axial strain of the cylinder vs impact time.*

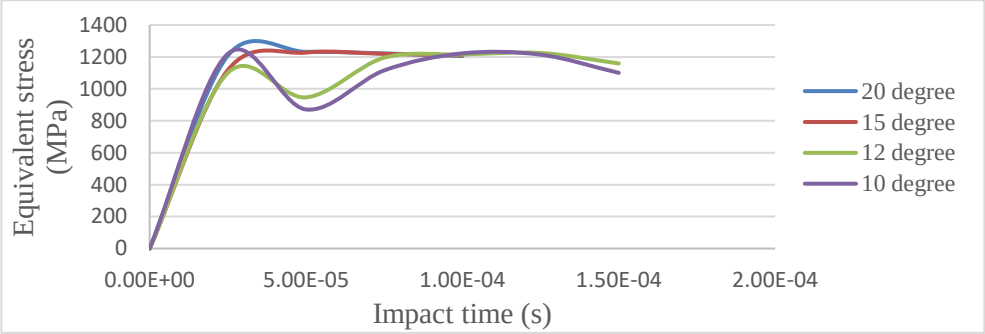

Hình 10. *The equivalent stress at the position B of the cylinder vs impact time.*

Figures 11 and 12 show the maximum radial strain, axial strain and the maximum equivalent stress of the cylinder tail for different piston taper angles.

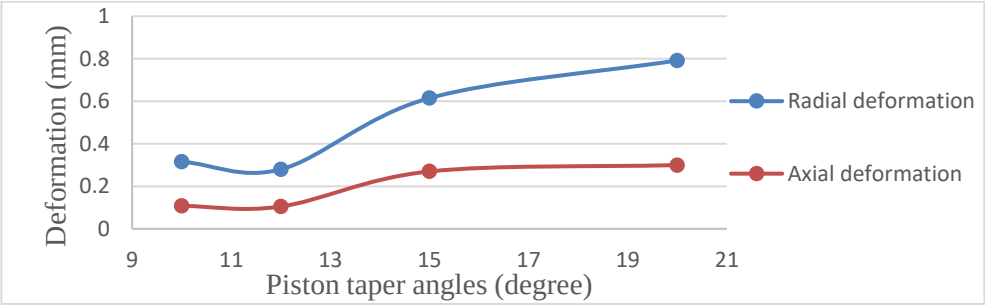

Figure 11. *Radial and axial deformation of cylinder tail vs piston taper angles.*

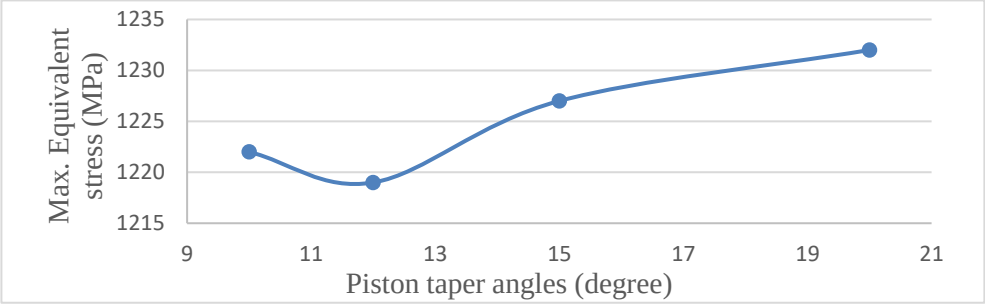

Figure 12. *Equivalent stress of cylinder tail vs piston taper angles.*

3.2. Discussion

From the result of the deformation, the equivalent stress of the cylinder tails as well as the impact process of the piston and cylinder. The main results of this study can be note as given below:

With the piston taper angle of 12°, the deformation and equivalent stress of the cylinder tail is minimal.

When the piston taper angle is changed to values less than the appropriate value, there will be a tendency to increase the equivalent stress in the cylinder tail at the first immediate impact, the radial deformation in this period tends to decrease, but increases the axial deformation. After this process, the deformation and equivalent stress of the cylinder tail will decrease until the bottom of the piston taper hit the bottom of the cylinder tail, at which time the deformation and equivalent stress of the cylinder tail will increase until the piston stops.

When the piston taper angle is changed to values greater than the appropriate value, at this time the impact will mainly be the impact between the bottom of the piston taper with the cylinder tail surface, the equivalent stress and deformation increase continuously until the piston stops.

3.3. Experimental results

Experiments using 5 samples with piston taper angle of 12°, cylinder taper angle of 20° have been carried out for the simulation results confirmation. The results of cylinder tail deformations are shown in table 4 and figure 13.

Table 4.*Cylinder tail deformation.*

Nº	Number of samples	Radial Deformation (mm)	Axial Deformation (mm)
1	1	0.3	0.15
2	2	0.27	0.13
3	3	0.25	0.1
4	4	0.24	0.11
5	5	0.21	0.1

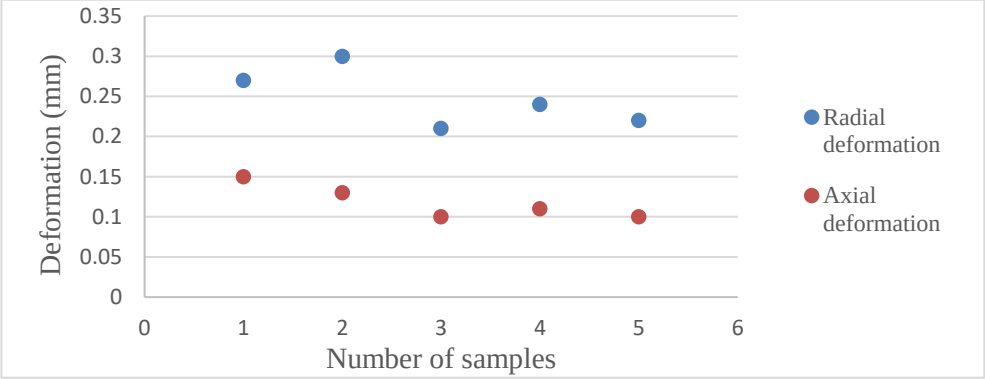

Figure 13. *Experimental results.*

3.4. Comparison of simulation and experimental results

Figure 14 presents comparison of the simulation and experimental results of the radial deformations, axial deformations of the cylinder tail in the case of 12° piston taper angle and 20° cylinder tail taper angel. The results of the simulation agree very well with the experimental results. The the difference between an experimental and theoretical value can be explained by the following reasons:

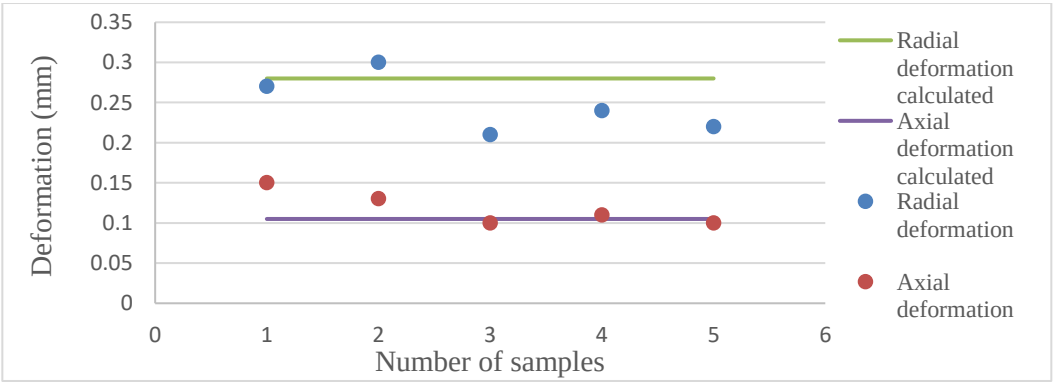

Figure 14. *Comparison of simulation and experimental results.*

The manufacturing dimensions of the pistons and cylinders have tolerances, while the dimensions of the simulation model are the nominal dimensions;

Material properties of the model have errors compared with the material manufactured of the pistons and cylinders;

Measurement error during measurement of experimental results.

4. CONCLUSIONS

The simulation model using Ansys explicit dynamic is built for solving the impact between the pison and the cylinder tail of the single use piston and cylinder system.In this article, the taper angle of cylinder tail is 20° and the taper angle of piston is changing from 10^o to 20^o. All dimensions of piston and cylinder tail are according to basic tactical specifications and sketchs.

The model using uniform three-dimensional solid elements and the Johnson cook strength model of material properties. Analysis of the impact between the pison and the cylinder tail is presented in this paper to determine the suitable value of the taper angle of single use piston. The radial, axial deformations, equivalent stress of the cylinder tail are explained clearly and the suitable taper angle of the piston has been determined, which is 12^o.

Analysis results of experiments are introduced in this paper to investigate the calculation results of 12^o taper angle of piston. Comparison of simulation results using ansys explicit dynamic and experimental results given by single use piston and cylinder system test confirm that all results of simulation agree with results of expreimental very well.

In order to match the manufacturing technology, the suitable tapper angle of the piston is always a range of values that also explains the method of selecting research values of the piston taper angle in this article. In this case, the suitable tapper angle of the piston is determined in the range from 10^o to 14^o. The results of the article are applied to manufacturing and testing 82 mm silent mortar systems.

REFERENCES

[1]. Siti Nurul, Yutaka Asako, Tan Lit, Nor Azwadi. *"Piston Surface Pressure of Piston- Cylinder System with Finite Piston Speed."* Journal of Advanced Research in Fluid Mechanics and Thermal Sciences 44, Issue 1, pp. 55-65, (2018).

[2]. Gruber, Christian, and Gary P. Morriss. "A Boltzmann equation approach to the dynamics of the simple piston." Journal of statistical physics 113, no. 1-2: 297-333, (2003).

[3]. https://soha.vn/sung-coi-va-dan-coi-triet-am-50-mm-viet-nam-co-gi-dac-biet-20171114115337878.html.

[4]. R.D. Cook, D.S. Malkus, M.E. Plesha, R.J. Witt, Concepts and Applications of Finite Element Analysis, fourth ed., Wiley, (2001).

[5]. B.P. Sommeijer, Increasing the real stability boundary of explicit methods, Computers & Mathematics with Applications 19 (6), pp. 37–49, (1990).

[6]. C.D. Acosta, C.E. Mejía, Stabilization of explicit methods for convection diffusion equations by discrete mollification, Computers & Mathematics withApplications 55 (3), pp. 368–380, (2008).

[7]. ANSYS Inc. ANSYS Workbench User's Guide, Release R2020.1.

TÓM TẮT

Nghiên cứu và thiết kế góc côn của piston sử dụng một lần

Trong bài báo này, sử dụng phương pháp mô phỏng số kết hợp với thực nghiệm đã đưa ra thiết kế phù hợp nhất cho góc côn của piston trong hệ thống piston – xilanh sử dụng một lần. Quá trình nghiên cứu cho thấy, khi piston có góc côn là 12^o đối với thiết kế góc côn của đuôi xi lanh là 20^o cho kết quả biến dạng, ứng suất tương đươngcủa đuôi xi lanh là nhỏ nhất cũng như thời gian giảm vận tốc của piston là lớn nhất, từ đó làm tăng độ kín và giảm thiểu ảnh hưởng của va chạm giữa piston và xi lanh đến quá trình bịt kín và khả năng hoạt động tin cậy của hệ thống. Kết quả sau nghiên cứu được chứng minh bằng thực nghiệm, kết quả thực nghiệm cho thấy kết quả mô phỏng là tin cậy và có tính ứng dụng cao. Kết quả của bài báo được áp dụng vào chế tạo và thử nghiệm hệ thống cối triệt âm 82 mm.

Từ khóa: Piston sử dụng một lần; Pison – xi lanh; Góc côn; Xi lanh; Biến dạng.